Proceedings of the ASME 2014 12th Biennial Conference on Engineering Systems Design and Analysis
ESDA2014
June 25-27, 2014, Copenhagen, Denmark

ESDA2014-20489

CFD PARAMETRIC STUDY OF THE INFLUENCE OF NUMBER AND ARRANGEMENT OF MEAT CARCASSES IN THE THERMAL PERFORMANCE OF REFRIGERATION ROOMS - CASE STUDY

E. Bastos
University of Beira Interior
Covilhã, Portugal

P. D. Gaspar
University of Beira Interior
Covilhã, Portugal

P. D. Silva
University of Beira Interior
Covilhã, Portugal

ABSTRACT

This paper describes the numerical results of a CFD parametric studies of the influence on the thermal performance of a cold room by (1) the number and arrangement (n = 6, 9, 18, 30 and 40) of meat carcasses hanging in an airway; (2) the air temperature in the antechamber (T = 5ºC; 14ºC and 22ºC); and of (3) opening the door of the cold room. The case studies were tested in a real facility. A steady state 3D CFD model of the cold room is developed, allowing the detailed evaluation of the airflow and heat transfer for each case study. The thermal conduction within the meat carcasses is also predicted. The numerical predictions show that the average air temperature inside the cold room as well as the average carcass temperatures increase with the number of products and depend on the arrangement of the carcasses in the airway. A minimum space between carcasses is required to improve the refrigeration process. Similarly, the heat load of the cold room increases with the air temperature of the antechamber and when the door of the cold room is opened. The carcasses temperature profile becomes less uniform when the door is opened, being the temperature of carcasses located near the door strongly affected. These parametric studies allow to evaluate details of the air flow and heat transfer by convection and conduction inside goods that can contribute to the design of cold rooms in order to focus on the improvement of thermal performance and consequently of food safety and energy efficiency.

NOMENCLATURE

General

$C_{1\varepsilon}$, $C_{2\varepsilon}$,	Turbulence model constants.
C_p	Specific heat, [$J \cdot kg^{-1} \cdot K^{-1}$].
D_h	Hydraulic diameter, [m].
I_t	Turbulence intensity, [%].
S	Source term, [$W \cdot m^{-3}$]
T	Temperature, [K].
U	Velocity component, [$m \cdot s^{-1}$]
g	Gravitational acceleration, [$m \cdot s^{-2}$].
k	Turbulent kinetic energy, [$m^2 \cdot s^{-2}$].
n	number of carcasses.
p	Pressure, [Pa].
v	Average velocity, [$m \cdot s^{-1}$].
x, y, z	Spatial coordinates, [m].

Greek Symbols

Γ	Diffusion coefficient.
β	Thermal expansion coefficient [K^{-1}].
ε	Dissipation rate of k, [$m^2 \cdot s^{-3}$].
ϕ	General variable.
μ	Dynamic viscosity, [$N \cdot s \cdot m^{-2}$]
ρ	Density, [$kg \cdot m^{-3}$].
σ	Prandtl number.

Subscripts

0	Operating.
ext	External.
i	Component of cartesian directions.
k	index.
t	Turbulent.
ϕ	General.

Abbreviation

2D	Two-dimensional.
3D	Thee-dimensional.
BC	Boundary Condition.
CFD	Computational Fluid Dynamics.
DAG	Discharge air grille.
PBP	Perforated back panel.
RAG	Return air grille.

INTRODUCTION

The main goal of this paper is to improve the thermal performance of cold rooms, broadly used in agrifood industries for meat storage, in order to increase the energy efficiency in this industry. In cold storage is important to ensure the correct

air distribution inside the cold chamber and to reduce the infiltration of warm air, from outside, due to door openings.

A CFD parametric study of a real cold room for meat storage is developed. The parametric study involves the number and displacement of meat carcasses, temperature of antechamber and an open/close door situation.

There are many numerical studies describing the thermal performance of cold chambers. Hoang *et al.* (2000) developed a numerical study of the airflow in a cold chamber using CFD. The authors assumed a steady state incompressible fluid model, based in Reynolds and Navier Stokes equations. The turbulence model used was the *k-ε* model. The renormalized model (RNG) was also tested. The model was validated, according to experimental data acquired. The relative error of air velocity was about 26%. The use of RNG model did not improve the numerical predictions. Sajadiye *et al.* (2012) validated a three-dimensional (3D) model of a cold chamber fully loaded in order to predict its thermal performance. The cold air was discharged with high velocity in the chamber's floor. The results shown a decrease of products temperature from 14,9ºC to 13,1ºC in a vertical plane, and a decrease of 16,8ºC to 10,7ºC in a horizontal plane. Nahor *et al.* (2005) developed a 3D transient model to evaluate air temperature, velocity and its distribution in a cold room. The cold chamber was tested for two case studies: empty and full of goods. The *k-ε* turbulence model was used with standard wall functions type. The model was validated with the experimental data of air velocity and temperature. The relative error of air velocity achieved for the empty case study was 22%, while for full case study it achieved 20%. Tavares *et al.* (2012) evaluated the air distribution in a partially loaded cold room using a CFD model. The main goal was to test the effect of a deflector in the air distribution. The turbulence model chosen was the *k-ε* RNG model. Experimental results validated the developed model. The authors verified that the deflector improves air circulation. Ho *et al.* (2010) investigated the airflow inside a cold chamber with 2D and 3D steady state models. The authors developed a parametric study which changed different parameters, such as discharge air velocity and the location of evaporators. The results showed an improvement in air distribution and temperature due to the increase of air velocity. Muñoz *et al.* (2012) modelled the air distribution in a dry ham unit. The turbulence model used was the *k-ε* model. The authors tested 3 cases: (1) air velocity: 18 m/s; (2) discharge and return air velocities respectively: 20 m/s and 15 m/s; (3) discharge and return air velocities respectively: 22 m/s and 10 m/s. The last case study was the most reliable. Foster *et al.* (2002) developed a CFD transient model with the main goal to predict the air infiltration from outside air. The model was validated by comparison with the experimental results of air velocity. The computational mesh was improved until convergence was achieved. A total of 113.188 tetrahedral elements were obtained, with 21.626 nodes. The *k-ε* turbulence model was used. The time simulation considered for the door opening was 30 sec. The flexibility provided by numerical models is an advantage to simulate real phenomena. Campos *et al.* (2013) analyzed the thermal performance of a cold room for meat storage, using experimental test and numerical tools. An experimental test was conducted to evaluate the distribution of air velocity and temperature inside the cold room. Then a steady-state 3D CFD model was developed, which took the experimental results as boundary conditions. The numerical simulation allowed the analysis of the air distribution and heat transfer inside the cold room. The model was validated, which allowed the development of a parametric study. It considered different discharge air velocities and temperatures. The results showed that the refrigeration system was oversized. The current study is based on that work, where some changes are made and different parameters are analyzed in order to evaluate the thermal performance of the cold chamber.

This group of numerical case studies focus on the thermal performance of cold chambers, and confirms the relevance of developing even more studies in this field. Due to the inexistent studies concerning airways for meat transfer and storage, this paper reveals an important achievement in this field.

MATHEMATICAL AND NUMERICAL MODEL

Geometry

The development of the geometric model minimized the computational effort, without compromise the results accuracy. All bodies and components of the cold chamber were approximated to regular solids. The cold chamber in study has 10,0x6,0x3,2 m^3, and the ante chamber has 4,0x2,0x3,2 m^3. Figure 1 shows a general layout of the developed geometry.

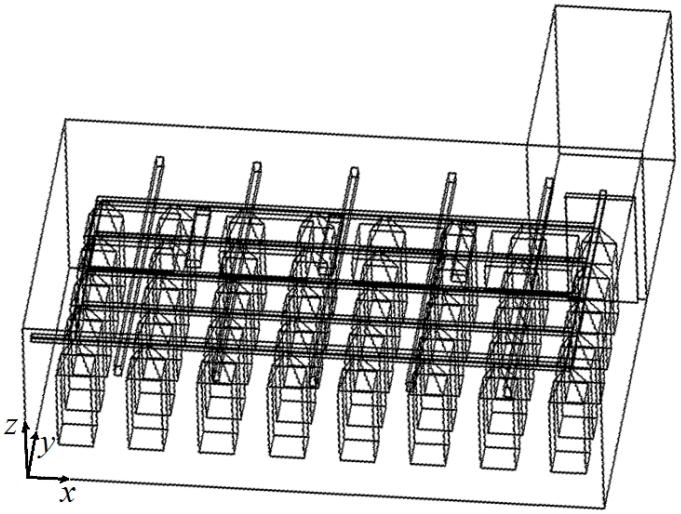

Figure 1- Layout of the studied cold room.

Computational mesh

The construction of the computational mesh consists in a division of the geometric domain, where the mathematical equations are resolved to simulate the studied phenomena. The mesh obtained in this work was based on tetrahedral elements. Instead of performing a mesh sensitivity analysis to evaluate

the balance between mesh quality and computational cost, the average Aspect Ratio and Skewness values were calculated for the different computational meshes developed along the model creation to ensure a reasonable mesh's quality. The final computational mesh presented respectively 1,862 and 0,229. Both values are considered good for tetrahedral elements. The mesh has 642.254 elements with 127.691 nodes.

Mathematical formulation

The air flow and non-isothermal heat transfer process are modelled by a 3D steady state model. The basic equations governing transport phenomena in the cold room are continuity, momentum and energy Ferziger and Perić (2002). These governing equations for the averaged flow of an incompressible fluid can be written in the general form by Eq. (1) for a dependent variable ϕ (=1 for the continuity equation, = v_i for momentum equations, and = T for energy equation.

$$\frac{\partial}{\partial x_k}\left(\rho v \phi - \Gamma_\phi \frac{\partial \phi}{\partial x_k} \right) = S_\phi \quad (1)$$

For application on the computational domain, the airflow modelling is coupled to products modelling, where within the latter region the convection term is neglected.

Air is considered as incompressible fluid. One way to model the variation of fluid density is to take the densities difference in the flow taking into account the momentum equation, i.e. the Boussinesq model. The Boussinesq model given by Eq. (2) is valid for small variations in density, i.e., for small variations in temperature, which is the current case.

$$\left(\rho - \rho_0\right)g = -\rho_0 \beta \left(T - T_0\right)g \quad (2)$$

The operating temperature, T_0, and corresponding density, ρ_0, are set to the values that ensure meat safety (T_0 = 4ºC and ρ_0 = 1,268 kg·m^{-3}).

The energy equation is developed as function of temperature in steady state with constant specific heat. Further simplifications are accomplished by neglecting viscous dissipation due to flow characteristics. The influences of air humidity and thermal radiation are not considered in this model.

The turbulence is modelled by the two equation k-ε model (Launder and Spalding, 1974), due its ability to model turbulence in a wide range of flows with minimum coefficients adjustment and also for its relatively simple formulation. The set of model equations shown in Eq. (3) and Eq. (4) is suitable for fully turbulent flow.

$$\frac{\partial \rho k}{\partial t} + div(\rho U k) - div\left[\left(\mu + \frac{\mu_T}{\sigma_k}\right) grad(k)\right] = P - \rho\varepsilon \quad (3)$$

$$\frac{\partial \rho \varepsilon}{\partial t} + div(\rho U \varepsilon) - div\left[\left(\mu + \frac{\mu_T}{\sigma_\varepsilon}\right) grad(\varepsilon)\right] = C_{1\varepsilon}\frac{\varepsilon}{k}P - C_{2\varepsilon}\rho\frac{\varepsilon^2}{k} \quad (4)$$

To account for viscous effects and high gradients in proximity of walls, the turbulence model equations are used in conjunction with empirical wall functions. The complete description and implementation details of wall functions in turbulence models can be found in Rodi (1980).

The solid zone is considered as the control volumes of the parallelograms that simulate the meat carcasses (see Fig. 1), Only the heat transfer mechanism by conduction is considered in this zone. Table 1 shows the thermophysical properties of meat carcasses (ASHRAE, 2006). An initial temperature of carcasses was set to T = 5ºC, as being the body temperature of carcasses entering the cold chamber.

Table 1- Termophysical properties of carcasses.

Parameter	Value
Density	ρ = 1090 kg·m^{-3}
Thermal conductivity	k = 0,506 W·m^{-1}·K^{-1}
Specific heat	C_p = 3240 J·kg^{-1}·K^{-1}

Numerical model

The mathematical model is a set of coupled non-linear partial differential equations, expressing mass, momentum and energy conservation which should be simultaneously and interactively solved. The present study makes use of a commercial CFD code Fluent for solution of this set of equations. The computational procedure used is based on a numerical iterative process using the SIMPLEC (*Semi-Implicit Method for Pressure-Linked Equations Consistent*) algorithm for pressure-velocity coupling (Patankar, 1980). The equations were discretized in the control volume form using different differencing schemes. Field variables (stored at cell centres) are interpolated to the faces of the control volumes with the Second-Order Upwind scheme. The interpolation scheme used for calculating cell-face pressures was selected was PRESTO! (*PREssure STaggering Option*).

Boundary conditions

Some values considered in this work, were defined from the experimental data obtained by Campos *et al.* (2013). Other parameters were chosen according to the existing literature.

This work used the analytical model developed by Foster *et al.* (2013) to obtain the boundaries conditions values, applied on chamber's walls, ceiling and floor (see Table 2).

Figure 2 shows the locations of the boundary conditions imposed in the model for all case studies.

1. Imposed heat flux in walls, ceiling and floor;
2. Outlet pressure in evaporator's return air grille (RAG);
3. Imposed velocity inlet in evaporator's discharge air grille (DAG);
4. Imposed heat flux from lighting.

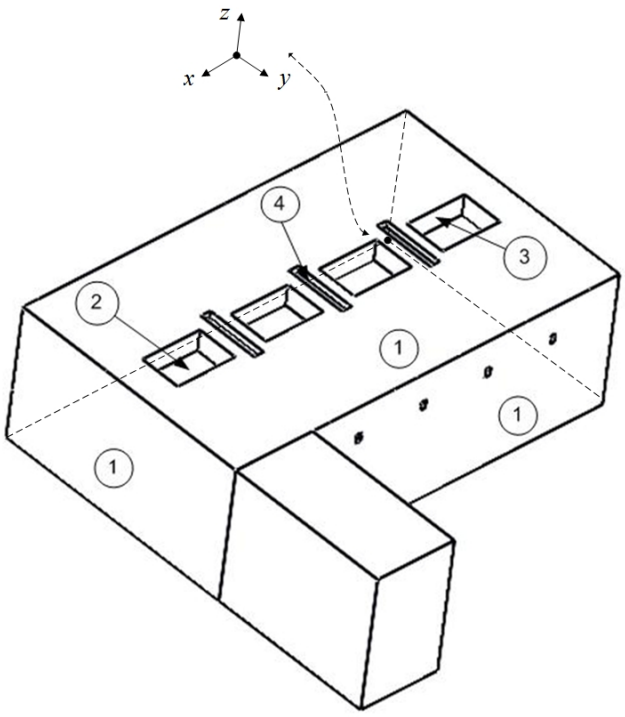

Figure 2- Location of main boundaries conditions.

To simulate the real phenomena, a thermal load was applied, in fourth condition to consider the chamber´s lightning. A thermal load of 1700 W was imposed.

Table 2- Thermal loads applied at boundary conditions.

Surface	Heat flux [$W \cdot m^{-2}$]
Wall 1	q_1 =6,69
Wall 2	q_2 =6,56
Wall 3	q_3 =16,00
Wall 4	q_4 =15,10
Ceiling	$q_{ceiling}$ =15,80
Floor	q_{floor} =35,20

A heat generation term S [$W \cdot m^{-3}$] was introduced in fluid zone, in order to simulate some loads as defrosting devices, fans and metabolic rate of workers. This term was evaluated according to the analytical model for heat flow calculation on cold stores exposed in Foster *et al.* (2013). This source term is obtained assuming a uniform distribution inside the cold store volume. This term is considered in the source term of Eq. (1).

Case studies are performed to evaluate the air temperature and velocity distributions inside the cold chamber depending on the:

Case study n.º 1: number and arrangement of carcasses inside the cold chamber. The carcasses control volumes are set to solid or fluid depending on the number of carcasses to be modelled. The initial temperature of the control volumes set as solid region to simulate carcasses is set to T = 5ºC. A heat generation term is imposed in the fluid zone of cold chamber volume.

Case study n.º 2: Antechamber air temperature. The antechamber control volumes are set to fluid. A heat generation term is imposed in the fluid regions of cold chamber and antechamber. The control volumes in the door between the two spaces are considered as solid zone, i.e., the door is closed.

Case study n.º 3: Opening the door between the cold chamber and antechamber: The control volumes in the door between the two spaces are considered as fluid zone, i.e., the door is open.

Turbulence parameters

In order to model the turbulent kinetic energy and its dissipation rate, two parameters were chosen: turbulence intensity, I_t, and hydraulic diameter, D_h. In Table 3 are shown the values of the boundaries conditions applied to DAG and RAG.

Table 3- Boundary conditions imposed at evaporator's grilles.

Parameter	Zone	
	Discharge	Return
Turbulence intensity	I_t = 5%	I_t = 10%
Hydraulic diameter	D_h = 0,353 m	D_h = 1,2 m
Temperature	T = 0 °C	T = 1,3 °C
Velocity / relative pressure	v = 3,6 $m \cdot s^{-1}$	p_r = 80 Pa

PARAMETRIC STUDIES

In this work different cases were studied. Case 1 studies the influence of load and arrangement of 6, 9, 18, 30 and 40 carcasses. In the second case the influence of antechamber's temperature (5 ºC, 14 ºC and 22 ºC) is investigated. Finally the third case verifies the impact from exterior air due to door openings. The number of carcasses, the air temperature variation of the antechamber and the air infiltration influence the heat generation term used in the fluid zone. For each case study, the values of the heat generation term are presented.

Influence of number and arrangement

The first case study evaluates the influence of the number and arrangement of carcasses inside the cold chamber on its air temperature and velocity distributions. In Table 4 are shown the heat generation term imposed in the model for each condition. This term also accounts for the initial thermal load of carcasses.

Table 4- Heat generation term according to carcasses' number.

Number of carcasses, n	6	9	18	30	40
Heat generation term, S [$W \cdot m^{-3}$]	10,09	10,19	10,49	10,94	11,34

In Fig. 3 is shown the air temperature field at the middle plane for a 6 carcass disposal, which shows the uniformity of air temperature inside the cold room and how heat is transferred into carcasses ensuring food safety. It´s visible the heat load of lights in zones under their location.

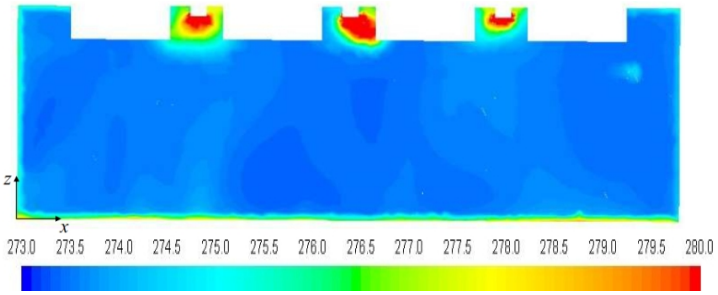

Figure 3- Air temperature field (K) for 6 carcasses in plane *x*-*z* at *y* = 3 m.

In Fig. 4, the numerical predictions of air velocity vectors in a half-height plane show the existence of vortices and recirculation zones generated by momentum promoted by the air flow from DAG. The location of the 9 carcasses inside cold chamber influence the vortices size. The empty zone of the cold chamber is the area where larger vortices phenomena occur.

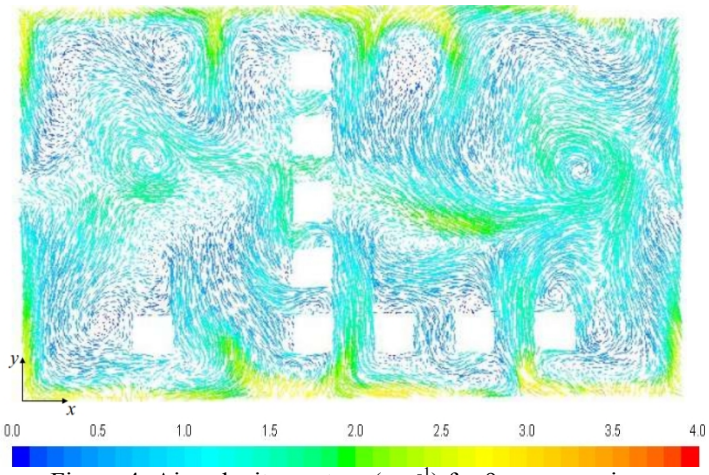

Figure 4- Air velocity vectors ($m \cdot s^{-1}$) for 9 carcasses in plane *x*-*y* at *z* = 1,1 m.

In Fig. 5, the number of carcasses increases to 18 which affects the air distribution inside the cold room. Once again, the empty space allows the formation of vortices.

The average air temperature with 30 carcasses increases slightly as shown in Fig. 6. The uniformity of air temperature field is affected by the obstruction of air flow caused by the location of carcasses. It is predicted a reduction of the average air velocity due to the greater obstruction and space occupied by carcasses. Still, the maximum temperature predicted does not represents a threat to food safety of the meat products.

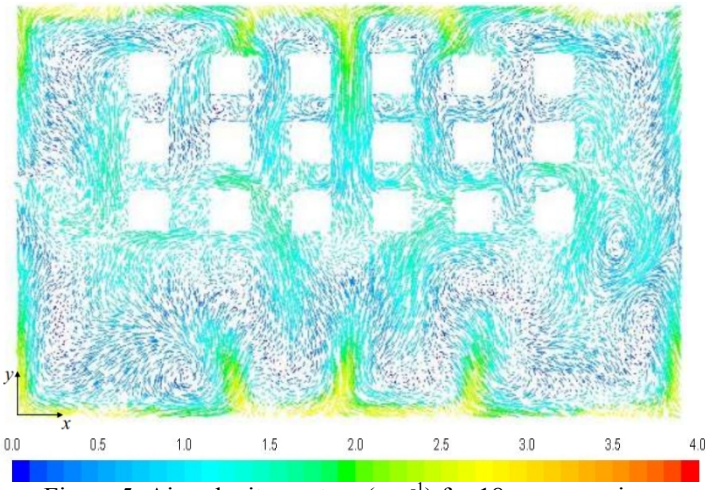

Figure 5- Air velocity vectors ($m \cdot s^{-1}$) for 18 carcasses in plane *x*-*y* at *z* = 1,1 m.

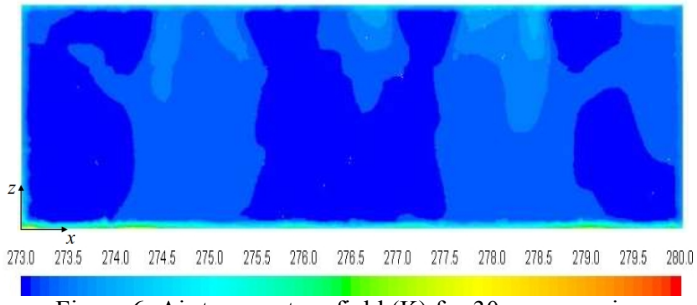

Figure 6- Air temperature field (K) for 30 carcasses in plane *x*-*z* at *y* = 5 m.

The increase of carcasses up to 40 blocks the air flow which has a negative effect on the effectiveness of the refrigeration process as shown in Fig. 7.

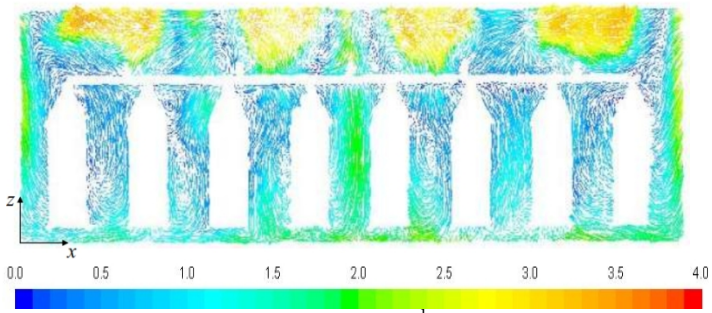

Figure 7- Air velocity vectors ($m \cdot s^{-1}$) for 40 carcasses in plane *x*-*z* at *y* = 5 m.

Influence of the air temperature in the antechamber

For case study n.º 2 were considered 40 carcasses store inside de cold chamber. The heat generation term was recalculated to account for the thermal load resulting from the air temperature variation in the antechamber. The values of heat generation term used in this case study are shown in Table 5.

Table 5- Heat generation term according to the antechamber air temperature.

Antechamber air temperature, T_{ext} [ºC]	5	14	22
Heat generation term, S [W·m^{-3}]	7,76	11,34	18,5

In Fig. 8, the air temperature field for 5ºC shows that the temperature inside the cold chamber is near 0ºC. The "hot spots" inside the cold chamber are related to large occupancy of the cold chamber with carcasses, which reduces the refrigerated air flow.

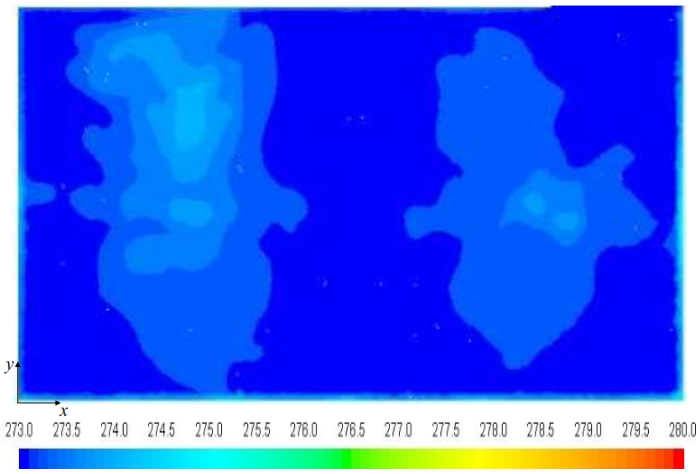

Figure 8- Air temperature field (K) for antechamber with air temperature of 5 ºC (plane x-y at z = 1, 1 m).

In Fig. 9, the increase of antechamber temperature up to 14 ºC reveals a warmer zone inside the cold chamber. This warmer zone is located in the vicinity of the wall separating the cold chamber from the antechamber.

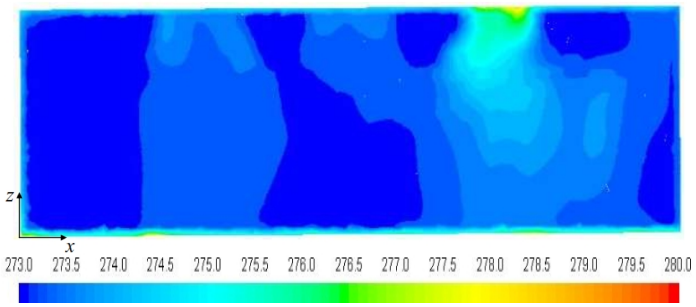

Figure 9- Air temperature field (K) for antechamber with air temperature of 14 ºC (plane x-z at y = 5 m).

The effect of heat load of lightning is predicted in Fig. 10 as the antechamber air temperature rises to 22 ºC. Some zones near the wall separating cold chamber and antechamber are near the food safety limit.

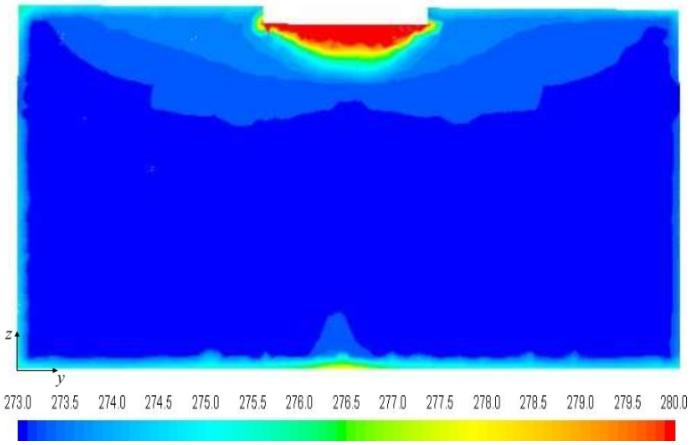

Figure 10- Air temperature field (K) for antechamber with air temperature of 22 ºC (plane y-z at x = 5 m).

Influence of door opening

For the case study n.º 3, were again considered 40 carcasses stored inside de cold chamber. The heat generation term in cold chamber and antechamber volumes were calculated to account for the thermal load resulting from the air infiltration. The values of the heat generation term considered were 8,36 W·m^{-3} for the cold room volume and 19,5 W·m^{-3} for the antechamber volume. The air velocity in the antechamber was considered null, meaning that only natural convection occurs. The predictions of air velocity vectors shown in Fig. 11, reveal the thermal entrainment that occurs between cold chamber and antechamber, as well as the high exposure of carcasses next door zone to outside air. This higher air temperature compromises food safety limit, as Fig. 12 suggests.

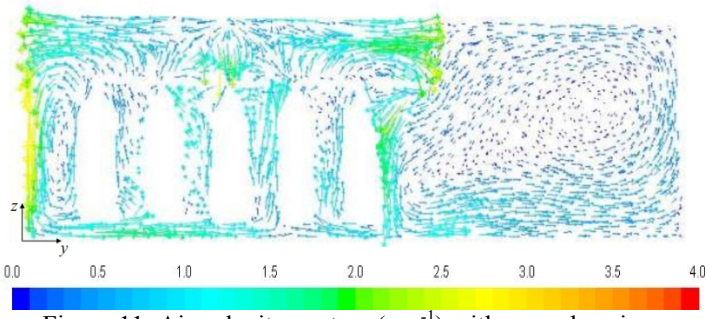

Figure 11- Air velocity vectors (m·s^{-1}) with open door in plane y-z at x = 9,3 m.

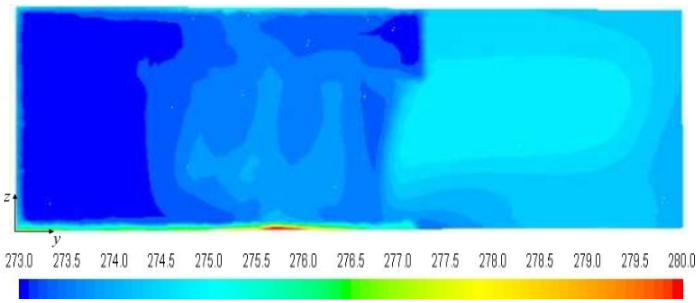

Figure 12- Air temperature field (K) with open door in plane *y*-*z* at *x* = 9,3 m.

RESULTS AND DISCUSSION

The numerical predictions reveal air stagnation between carcasses. This air in recirculation doesn't exchange any heat with the carcasses. In the various models simulated, was verified a negative impact due to air way and beams. These structural elements disturb the air path. The bovine carcasses under the return grilles were, as expected, more often refrigerated. Although this location is the best to cool the carcasses, the main objective is to ensure this condition in all locations inside the cold chamber. Figure 13 represents the average air temperature inside the cold room according to the number of bovines carcasses stored. Generally, the air temperature increases with the number of carcasses.

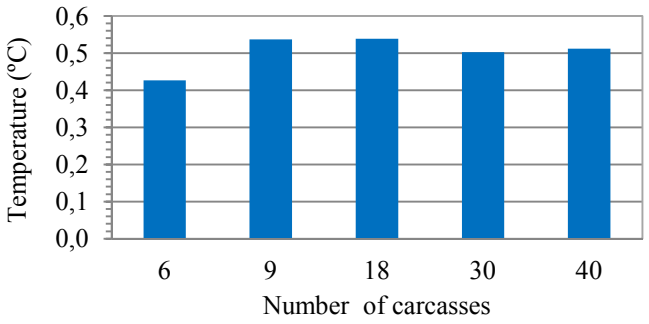

Figure 13- Average air temperature (ºC) with different carcasses number stored.

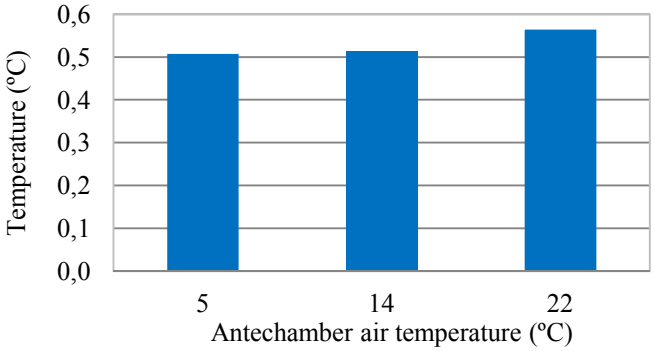

Figure 14- Average air temperature (ºC) of the cold room according to antechamber's air temperature.

The antechamber simulations confirm the importance of climatic rooms. The results shown in Figure 14 prove that the antechamber's air temperature influences the thermal performance of the cold room.

CONCLUSIONS

This work involved the development of a steady-state 3D CFD modelling of an industrial meat cold room where carcasses are transferred and stored in airways. The parametric studies were carried out to evaluate the influence on the thermal performance of the cold room by the number and arrangement of carcasses stored in the airway, by the value of air temperature in the antechamber, and by the thermal entrainment due to door opening to the antechamber. Generally, the air temperature inside the cold chamber increases with the number of carcasses mainly due to the obstruction of the refrigerated air flow by the number and location of carcasses. Also, the increase of the antechamber's air temperature has a negative impact on the thermal performance of the cold room. The opening of doors due to load and unload of the cold chamber also considers a significant effect of thermal performance and food safety due to the thermal entrainment with outside air.

A suitable space must exist between carcasses to promote the correct air circulation. The airways and beams should not perturb the air flow from discharge and return air grilles.

The proper design of agrifood facilities for cold storage is fundamental not only for the food safety but also for low electrical energy consumption. CFD parametric studies can help to analyze details in the airflow and heat transfer inside these facilities and to propose some specific retrofitting options. This particular CFD model has the advantage of simulating a cold chamber where meat carcasses are arranged along an airway that facilitates the carcasses transfer and storage, but, if not well design, can perturb the refrigerated airflow and thus reducing the thermal performance and consequently the food safety.

ACKNOWLEDGMENTS

This study is framed in the anchor-project "InovEnergy - Energy Efficiency in Agro-Industrial Sector" activities encompassed within Action Programme of InovCluster: Association of Agro-Industrial Cluster of Center region. The study was funded by the National Strategic Reference Framework (QREN 2007-2013) - COMPETE/POFC (Operational Programme for Competitiveness Factors), SIAC - Support System for Collective Actions: 01/SIAC/2011, Ref: 18642).

REFERENCES

[1] Hoang, M.L., Verboven, P., De Baerdemaeker, J., Nicolai, B.M. (2000), "*Analysis of the air flow in a cold store by means of computational fluid dynamics*", International Journal of Refrigeration 23(2), pp. 127–140.

[2] Sajadiye, S.M., Ahmadi, H., Hosseinalipour, S.M., Mohtasebi, S.S., Layeghi, M., Mostofi, Y., Raja, A. (2012), *"Evaluation of a Cooling Performance of a Typical Full*

Loaded Cool Storage Using Mono-scale CFD Simulation", Modern Applied Science 6(1), pp. 102-119.
[3] Nahor, H.B., Hoang, M.L., Verboven, P., Baelmans, M., Nicolai, B.M. (2005), *"CFD model of the airflow, heat and mass transfer in cool stores"*, International Journal of Refrigeration 28(3), pp. 368–380.
[4] Tavares, N., Garcia, J., Cerdeira, R., Coelho, L. (2012), *"Studying strategies for air distribution inside a refrigeration chamber under partial load conditions"*, CYTEF-2012. VI Congreso Ibérico y IV Congreso Iberoamericano de Ciencias y Técnicas del Frío.
[5] Ho, S.H., Rosario, L., Rahman, M.M. (2010). "*Numerical simulation of temperature and velocity in a refrigerated warehouse*", International Journal of Refrigeration 33(5), pp. 1015–1025.
[6] Muñoz, I., Comaposada, J., Stawczyk, J., Krempski-Smejda, M. (2012), *"Simulación de la fluidodinámica de un secadero de embutidos mediante CFD"*, CYTEF-2012. VI Congreso Ibérico y IV Congreso Iberoamericano de Ciencias y Técnicas del Frío.
[7] Foster, A.M., Barrett, R., James, S.J., Swain, M.J. (2002), "*Measurement and prediction of air movement through doorways in refrigerated rooms*", International Journal of Refrigeration 25.
[8] Campos, R., Bastos, E., Gaspar, P.D., Silva, P.D. (2013), *"Experimental study and numerical modeling of the thermal performance of cold rooms for storage of meat products",* 8th World Conference on Experimental Heat Transfer, Fluid Mechanics, and Thermodynamics June 16-20, 2013, Lisbon, Portugal.
[9] Ferziger, J.H., Perić, M. (2002), "*Computational methods for fluid dynamics - 3rd ed*", Berlin, Germany: Springer-Verlag.
[10] Launder, B.E., Spalding, D.B. (1974), "*The numerical computation of turbulent flows*", Computer Methods in Applied Mechanics and Engineering, 3(2), 269-289.
[11] Rodi, W. (1980), "*Turbulence models and their application in hydraulics. A state of the art review*", International Association for Hydraulics Research.
[12] ASHRAE (2006), "ASHRAE Handbook: Refrigeration", American Society of Heating, Refrigerating and Air-Conditioning Engineers, Inc.
[13] Patankar, S.V. (1980), "*Numerical Heat Transfer and Fluid flow*", Hemisphere Publishing Corporation.
[14] Foster, A., Zilio, C., Corradi, M., Reinholdt, L., Evans, J. (2013) Evans, J.A., Foster, A.M., Huet, J.-M., Reinholdt, L., et al, "*Specific energy consumption values for various refrigerated food cold stores*", Energy and Buildings (2013), http://dx.doi.org/10.1016/j.enbuild.2013.11.075